Catalysis Communications 52 (2014) 22–25

Contents lists available at ScienceDirect

Catalysis Communications

journal homepage: www.elsevier.com/locate/catcom

Short Communication

Effective catalytic hydrodechlorination of 4-chlorophenol over a Rh immobilized on amine-functionalized magnetite nanoparticles in aqueous phase

Guangyin Fan [a,*], Yanlin Ren [a], Weidong Jiang [b], Chenyu Wang [c], Bin Xu [b], Fuan Liu [b]

[a] Chemical Synthesis and Pollution Control, Key Laboratory of Sichuan Province, College Of Chemistry and Chemical Industry, China West Normal University, Nanchong 637002, China
[b] Key Laboratory of Green Catalysis of Sichuan Institute of High Education, Zigong 643000, China
[c] Department of Chemistry, State University of New York at Binghamton, Binghamton, NY 13902, USA

ARTICLE INFO

Article history:
Received 28 February 2014
Received in revised form 3 April 2014
Accepted 5 April 2014
Available online 13 April 2014

Keywords:
Hydrodechlorination
4-Chlorophenol
Magnetite
Rhodium

ABSTRACT

Amine-functionalized magnetite nanoparticles synthesized from a facile one-pot template-free method were applied as carriers for depositing Rh nanoparticles using $RhCl_3$ as the precursor. The as-prepared nanocomposites were applied for the hydrodechlorination of 4-chlorophenol at room temperature and atmospheric pressure. A complete conversion of 4-CP was obtained with the generation of phenol, cyclohexanone as the main products. The excellent catalytic activity, stability and recyclability of the catalyst were probably contributed to the functionalities of amine groups for stabilizing the Rh nanoparticles and the magnetic effect of Fe_3O_4 support during consecutive recycling of the catalyst.

© 2014 Elsevier B.V. All rights reserved.

1. Introduction

Chlorophenols are of great concern not only because of their usefulness as end products or intermediates for the synthesis of herbicides, dyes, and plant growth regulators but also due to their strong toxicity and potential accumulation in the environment [1–3]. Among the techniques that have been applied to deal with these compounds, catalytic hydrodechlorination (HDC) without imposing any extra contamination or producing hazardous byproducts is recognized as an effective approach of detoxifying wastewater containing chlorophenols [4]. As such, a wide variety of heterogeneous catalysts have been developed for HDC, among which noble metals such as Rh, Pt and Pd exhibit relatively high activities and stabilities for this reaction. Particularly, Rh catalysts with the advantages of high catalytic property, resistance to the attack of acid and base, and relative stability under severe conditions have been intensively investigated with the aim of producing high valued products such as cyclohexanol and cyclohexanone. Therefore, the HDC of chlorophenols catalyzed by Rh catalysts is considered as the most promising pathway for detoxifying chlorophenols from the environmental point of view [5].

Regarding the supports, a variety of solid materials such as active carbon [6–9], Al_2O_3 [8–13], and ZrO_2 [14] have been developed to immobilize noble metal nanoparticles for HDC reaction, among which Al_2O_3 and active carbon are commonly investigated. However, the catalytic property of the catalysts reported in the literature was not satisfied enough due to the possible deactivation of the catalysts and leaching of the active sites during the recycling. Therefore, it still remains as a tremendous challenge to seek stable and recyclable catalysts for the conversion of chlorinated phenols under mild conditions. In recent years, functionalized magnetic materials have emerged as applicable alternatives to the conventional materials, which offer the advantage of being magnetically separable without filtration [15]. Particularly, the functional groups such as NH_2 groups on the surface of the supports are benefitted to inhibit the agglomeration of nanoparticles and further improve the activity and stability of the catalysts through anchoring the metal ion and improving the dispersing ability [16]. Therefore, the introduction of functionalized magnetic nanocrystals as solid matrices have been widely applied in a range of organic transformations such as oxidation [17], hydrogenation [18–20] and C – C coupling reactions [21,22]. However, as far as we are concerned, rarely any literature about the application of noble metal nanoparticles deposited on the amine functionalized Fe_3O_4 supports as catalysts for the HDC reaction has been reported.

To this end, a facile approach to obtain Rh nanoparticles immobilized on 1,6-hexanediamine-functionalized Fe_3O_4 support has been proposed in this article. Subsequently, the as-prepared nanocomposites were examined in the catalytic HDC of 4-CP, exhibiting excellent activity, stability and recyclability. We ascribe the extraordinary catalytic property to

* Corresponding author. Tel./fax: +86 817 2568081.
E-mail address: fanguangyin@cwnu.edu.cn (G. Fan).

http://dx.doi.org/10.1016/j.catcom.2014.04.006
1566-7367/© 2014 Elsevier B.V. All rights reserved.

the well-dispersed Rh particles, anchoring function of NH_2 group and magnetic property of Fe_3O_4 support.

2. Experiment

2.1. Synthesis of $Rh/NH_2–Fe_3O_4$

The amine-functionalized Fe_3O_4 was prepared by the solvothermal method reported by Li and co-workers [23]. In a typical procedure, 1,6-hexanediamine (6.5 g), anhydrous sodium acetate (2.0 g) and $FeCl_3 \cdot 6H_2O$ (1.0 g) were added into a 30 mL ethylene glycol under vigorous stirring at 50 °C until a transparent solution was formed. Then the as-prepared solution was transferred into a 100 mL Teflon-lined autoclave and the temperature was kept at 200 °C for 6 h. After cooling down to room temperature, the black solid was separated from the supernatant with a magnet and washed with deionized water and ethanol in order to remove the solvent and unbound 1,6-hexanediamine. The black solid was finally dried at 50 °C under vacuum for 12 h.

2.2. Synthesis of $Rh/NH_2–Fe_3O_4$

The catalyst $Rh/NH_2–Fe_3O_4$ was fabricated as follow: $NH_2–Fe_3O_4$ (0.5 g) was added into a 100 mL round-bottom-flask containing ethanol (50 mL) and was under ultrasonication for 30 min via an ultrasonic cleaning bath. Then the aqueous solution of $RhCl_3$ (1.6 mL, 32.1 mM) was dropped into flask and maintained under ultrasonication for 2 h. Afterwards, an excessive $NaBH_4$ solution was slowly added into above mixture at 0 °C under vigorous stirring. The black solid was collected with a magnet and washed with deionized water for three times, and finally dried under vacuum at 25 °C for 24 h. The weight percentage of Rh in the catalyst was determined by ICP analysis (1.0 wt.% $Rh/NH_2–Fe_3O_4$).

2.3. Catalyst characterization

Transmission electron microscopy (TEM) measurements were carried out on a JEOL model 2010 instrument operated at an accelerating voltage of 200 kV. The X-ray diffraction (XRD) patterns were obtained using a modern multipurpose theta/theta powder X-ray diffraction system, equipped with a fast linear detector. X-ray photoelectron spectroscopy (XPS, Kratos XSAM800) spectra were obtained by using Al Ka radiation (12 kV and 15 mA) as an excitation source (hv =1486.6 eV) and Au (BE Au4f = 84.0 eV) and Ag (BE Ag3d = 386.3 eV) as references. A Fourier transform infrared (FT-IR) spectrum was recorded with a Nicolet 6700 (resolution 0.4 cm^{-1}) infrared spectrometer.

2.4. Activity tests

The catalytic HDC of 4-CP was performed at room temperature in a 25 mL round-bottom-flask equipped with a hydrogen balloon. The reactor was immersed in a thermostatic water bath to keep the temperature constant. Typically, catalyst (5.0 mg) and 4-CP aqueous solution (0.5 g/L, 5.0 mL) were transferred into the flask. Next, the flask was vacuumed and flushed with pure hydrogen. The reaction time was accounted when the designated reaction temperature was reached and the stirring rate was adjusted to 1200 rpm. All liquid samples were analyzed by gas chromatography (Agilent GC-7890) with a FID detector and HP-5 supelco column (30 m × 0.25 mm, 0.25 μm film) and nitrogen as a carrier gas.

3. Results and discussion

The characterization of FT-IR spectrum was firstly introduced to confirm the formation of amine-functionalized Fe_3O_4. As illustrated in Fig. 1, the diffraction peak at 579 cm^{-1} was assigned to the Fe – O stretching which confirmed the formation of Fe_3O_4. In addition, the peaks at 1055, 1558, 1623, 3432 and around 2846–2923 cm^{-1} are

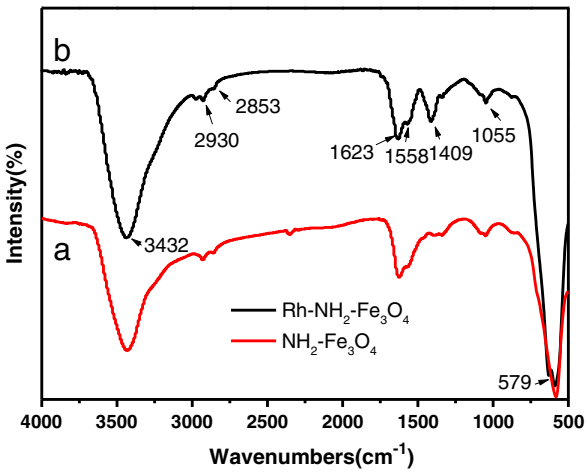

Fig. 1. FT-IR spectra of $NH_2–Fe_3O_4$ (a) and $Rh/NH_2–Fe_3O_4$ (b).

corresponding to the C – N stretching, N – H deformation and C – H stretching models of the alkyl chain, and the peak at 1409 cm^{-1} was attributed to the C – H symmetric blending vibration, which definitely confirmed the functionalization of Fe_3O_4 with 1,6-hexanediamine [16]. Furthermore, it should be noted that the deposition of Rh NPs on the $NH_2–Fe_3O_4$ did not result in the change of the spectrum compared with that of $NH_2–Fe_3O_4$.

The morphology of the catalyst $Rh/NH_2–Fe_3O_4$ was investigated and the results are illustrated in Fig. 2. As shown in Fig. 2a, the support $NH_2–Fe_3O_4$ was a quadrilateral sheet with parallel sides (approximate 20 nm) and truncation at the corners, which is different from the spherical $NH_2–Fe_3O_4$ as reported by Li et al. [23]. The corresponding high-resolution TEM (HRTEM) image provided more structural details about the $Rh–NH_2–Fe_3O_4$ nanocomposites. The obvious lattice fringes indicate a high crystallinity of the support Fe_3O_4. As illustrated in the inset of Fig. 2b, the diffraction pattern shows that the Fe_3O_4 support is projected along the [110] zone axis. Two spacings of 0.48 nm are found on the basis of a measurement on more than 12 adjacent lattice fringes, which are consistent with the $(\bar{1}1\bar{1})$ and $(1\bar{1}\bar{1})$ planes of Fe_3O_4 phase. As such, the growth direction of Fe_3O_4 was predicted to be $[\bar{1}1$ 0], which is perpendicular to the (111) close-packed plane.

The XRD patterns of $NH_2–Fe_3O_4$ and $Rh/NH_2–Fe_3O_4$ are shown in Fig. 3. The sharp and strong characteristic peaks of the support $NH_2–Fe_3O_4$ demonstrate that the as-prepared magnetite nanoparticles are well crystallized. The peaks located at 18.9°, 31.2°, 36.8°, 44.7°, 55.6°, 59.3°, and 65.1° matched well with (111), (220), (311), (400), (422), (511), and (440) Bragg diffractions of Fe_3O_4 (JCPDS no. 26-1136) respectively, confirming the formation of Fe_3O_4 crystalline phase. Besides, it can be seen that the XRD pattern has no apparent variations after the Rh NPs were immobilized on the magnetite, indicative of that the crystalline structure and domain of the magnetic support were well maintained. Unexpectedly, no diffraction signals for metallic Rh were observed in the pattern, which can be presumably attributed to the small particle size of Rh NPs on the support.

To provide more evidence of the presence of elemental Rh crystallites, XPS characterization of $Rh/NH_2–Fe_3O_4$ was carried out. XPS survey scan of the surface of the $Rh/NH_2–Fe_3O_4$ particles was firstly performed. As explicated in Fig. 4a, apart from the feature peaks of oxygen, carbon, nitrogen, and iron, rhodium was clearly detected, confirming the successfully immobilization of Rh on the surface Fe_3O_4. The further determination of electronic state of the Rh particles in the $Rh/NH_2–Fe_3O_4$ catalyst was achieved via a high resolution narrow scan. As elaborated in Fig. 4b, the binding energies of $Rh3d_{5/2}$ and $Rh3d_{3/2}$ level in $Rh/NH_2–Fe_3O_4$ composite are 308.6 and 313.3 eV, respectively, somewhat higher than the standard zero-valent state values, indicating the

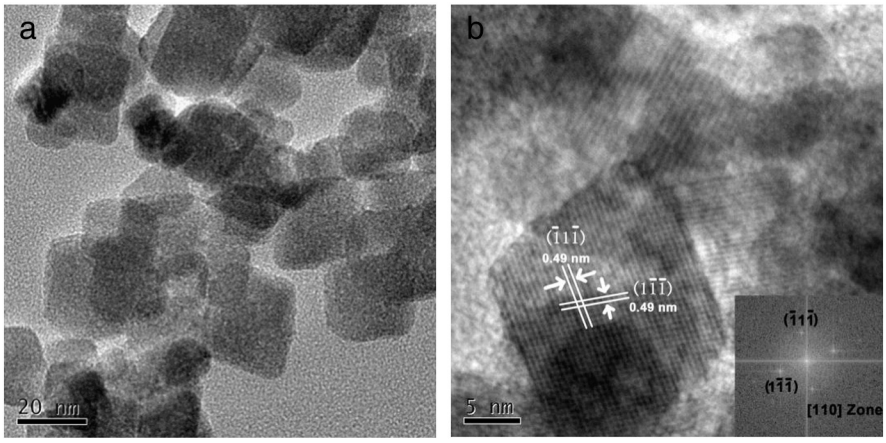

Fig. 2. TEM image of $Rh/NH_2–Fe_3O_4$ nanocomposites (a); HRTEM image showing the lattice fringes of $Rh/NH_2–Fe_3O_4$ nanoparticles with the inset of corresponding Fourier transformation pattern (b).

formation of the existence of electro-deficient Rh. This phenomenon was probably attributed to the interaction between the metallic Rh and the functionalized groups of support, in which the high electronegativity of nitrogen was supposed to decrease the electron density of Rh atoms in the catalysts [24]. Interestingly, the existence of electro-deficient Rh are benefitted to the catalytic performance of the catalysts for HDC reaction, [25] which was approved by the excellent catalytic activity of the $Rh/NH_2–Fe_3O_4$ at room temperature and balloon hydrogen pressure.

The catalytic properties of the as-synthesized $Rh/NH_2–Fe_3O_4$ nanocomposites were investigated using 4-CP as a model substrate. Phenol, cyclohexanol and cyclohexanone were detected as products during the HDC process. Simultaneously, HCl was also formed and dissolved in the aqueous phase. Blank test in the absence of metallic catalyst showed no occurrence of HDC reaction and thereby indicate that Rh species was the indispensable active component for such reaction. Additionally, negligible adsorption of 4-CP on the surface of catalysts was observed based on the adsorption experiments, showing that the removal of 4-CP was under chemical transformation. As shown in Fig. 5, a complete conversion of 4-CP was achieved within 90 min. Concerning the product distribution, the selectivity to phenol decreased from 79.8% with 15 min to 63.2% with 90 min, while an increase of the selectivity to cyclohexanone from 20.2% to 33.7% was obtained. Furthermore a trace amount of cyclohexanol (ca. 3.1%) was also detected in a reaction time of 90 min. Our results suggest that the removal of chloride process and reduction of the aromatic ring products (to generate cyclohexanol and cyclohexanone) simultaneously occurred. For comparison, the commonly used catalysts Rh/C, Rh/Al_2O_3 and the Rh/Fe_3O_4 without functional groups were prepared by a similar method with the same Rh loading of the $Rh/NH_2–Fe_3O_4$. The catalytic properties of these catalysts for the HDC of 4-CP under the same conditions were illustrated in Table 1. It can be seen that the catalysts Rh/C and Rh/Al_2O_3 showed moderate activity, while Rh/Fe_3O_4 exhibited the lowest activity toward the HDC reaction. The excellent catalytic activity of the catalyst $Rh/NH_2–Fe_3O_4$ was probably attributed to the functionalities of amine groups for

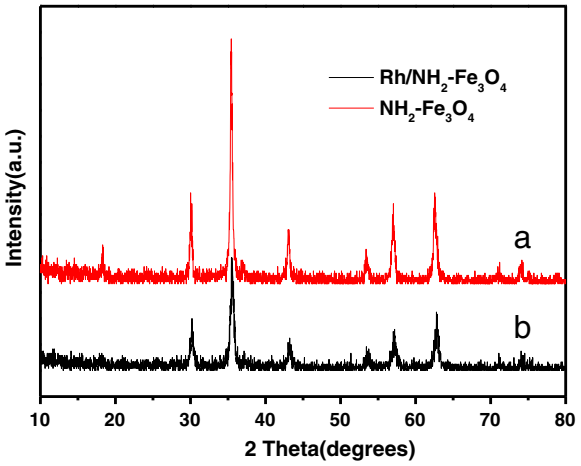

Fig. 3. XRD patterns of (a) $NH_2–Fe_3O_4$ and (b) $Rh/NH_2–Fe_3O_4$.

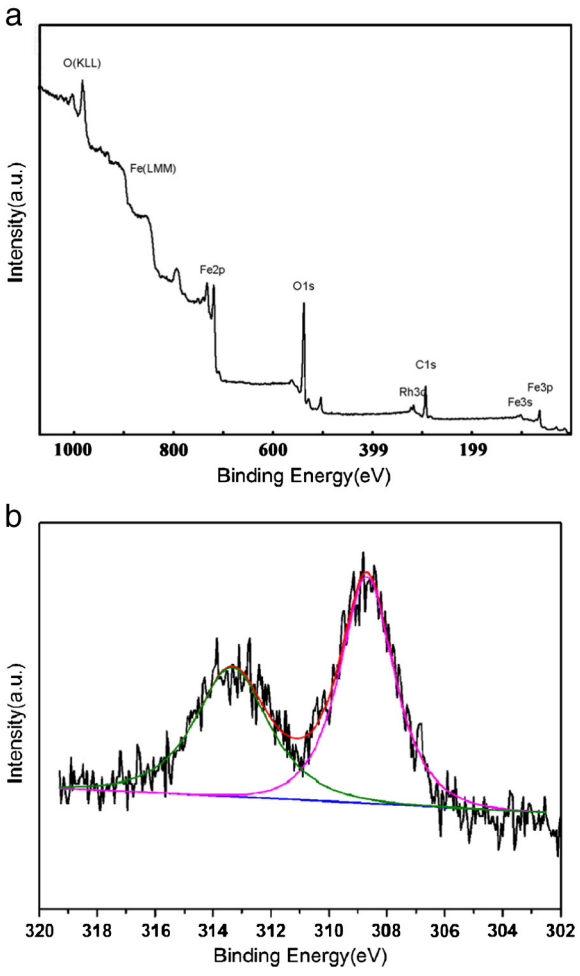

Fig. 4. XPS spectrum of the elemental survey scan of $Rh–NH_2–Fe_3O_4$ (a); XPS spectrum of the Rh in $Rh/NH_2–Fe_3O_4$ (b).

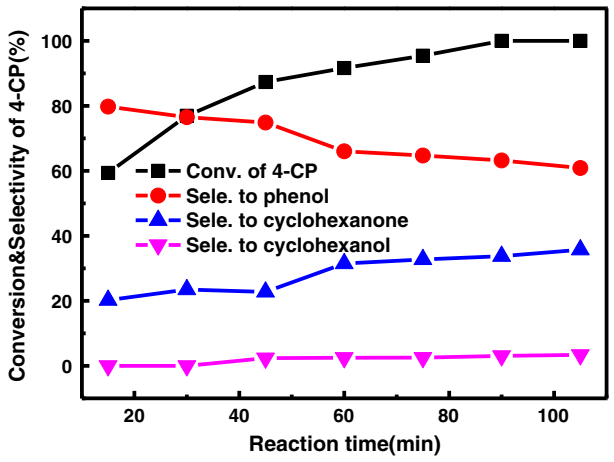

Fig. 5. HDC of 4-CP catalyzed by the catalyst $Rh/NH_2–Fe_3O_4$.

stabilizing the Rh nanoparticles avoiding the deactivation of Rh NPs during the HDC process.

The stability and recyclability of the catalyst $Rh/NH_2–Fe_3O_4$ were investigated through the collection of the catalyst by a magnet and re-applied it into the catalytic system for another 4 runs. The reusability tests (Table 1) showed that the conversion of 4-CP was still maintained at almost 90% without apparent deactivation in the 5th run, indicating that our novel structured catalyst possessed fine chemical stability. We ascribe the excellent stability to: 1) the strong anchoring effect of NH_2 which prevented the leaching of Rh; 2) the resistance to the attack of HCl offered by the basicity of amine groups; 3) the magnetism of Fe_3O_4 support, resulting in a facile collection of catalysts and immune from the loss usually caused by a mechanical recycling.

4. Conclusion

$Rh–NH_2–Fe_3O_4$ nanocomposites were prepared through the depositing Rh on the amine-functionalized Fe_3O_4 which was pre-synthesized via a solvothermal method using $FeCl_3$ as a precursor and 1,6-hexanediamine as a modifier. The nanocomposites exhibited excellent catalytic properties for the HDC of 4-CP at room temperature and atmospheric pressure, which was attributed to the anchoring function of amine groups on the surface of the catalyst that suppressed the loss of Rh particles during the HDC reaction.

Acknowledgment

This work was financially supported by the National Natural Science Foundation of China (21207109), the Applied Basic Research Programs of Science and Technology Department of Sichuan Province (No. 2014JY0107), and the Opening Project of Key Laboratory of Green Catalysis of Sichuan Institutes of High Education (No. LZJ1205).

Table 1
Catalytic properties of $Rh/NH_2–Fe_3O_4$ for 4-chlorophenol.[a]

Catalysts	Conversion (%)	Time (min)	Selectivity (%)		
			Phenol	Cyclohexanol	Cyclohexanone
Rh/C	78.6	90	87.4	0.2	18.4
Rh/Al_2O_3	50.3	90	74.0	1.1	24.9
Rh/Fe_3O_4	15.6	90	99.0	0	1.0
$Rh/NH_2–Fe_3O_4$	100	90	63.2	3.1	33.7
$Rh/NH_2–Fe_3O_4$	89.8	60	66.0	2.4	31.5
$Rh/NH_2–Fe_3O_4$[b]	89.7	60	68.3	2.0	29.7

[a] Reaction conditions: Catalyst: 5.0 mg; solvent: 5.0 mL (4-CP concentration, 0.5 g/L); reaction temperature: 25 °C; pressure: 1.0 atm.
[b] The catalyst was recycled five times.

References

[1] M.A. Keane, J. Chem. Technol. Biotechnol. 80 (2005) 1211–1222.
[2] M.A. Keane, Chem. Cat. Chem. 3 (2011) 800–821.
[3] Z.M. de Pedro, E. Diaz, A.F. Mohedano, J.A. Casas, J.J. Rodriguez, Appl. Catal. B Environ. 103 (2011) 128–135.
[4] G.-Q. Santiago, C.-L. Fernando, A.K. Mark, Nanotechnology 23 (2012) 294002.
[5] E. Diaz, A.F. Mohedano, J.A. Casas, L. Calvo, M.A. Gilarranz, J.J. Rodriguez, Appl. Catal. B Environ. 106 (2011) 469–475.
[6] C. Xia, J. Xu, W. Wu, X. Liang, Catal. Commun. 5 (2004) 383–386.
[7] C. Xia, Y. Liu, S. Zhou, C. Yang, S. Liu, J. Xu, J. Yu, J. Chen, X. Liang, J. Hazard. Mater. 169 (2009) 1029–1033.
[8] G. Yuan, M.A. Keane, J. Catal. 225 (2004) 510–522.
[9] G. Yuan, M.A. Keane, Appl. Catal. B Environ. 52 (2004) 301–314.
[10] S. Gómez-Quero, F. Cárdenas-Lizana, M.A. Keane, AIChE J. 56 (2010) 756–767.
[11] S. Gómez-Quero, E. Díaz, F. Cárdenas-Lizana, M.A. Keane, Chem. Eng. Sci. 65 (2010) 3786–3797.
[12] G. Yuan, M.A. Keane, Ind. Eng. Chem. Res. 46 (2007) 705–715.
[13] S. Gómez-Quero, F. Cárdenas-Lizana, M.A. Keane, Chem. Eng. J. 166 (2011) 1044–1051.
[14] Y. Shao, Z. Xu, H. Wan, H. Chen, F. Liu, L. Li, S. Zheng, J. Hazard. Mater. 179 (2010) 135–140.
[15] S. Shylesh, V. Schünemann, W.R. Thiel, Angew. Chem. Int. Ed. 49 (2010) 3428–3459.
[16] F. Zhang, J. Jin, X. Zhong, S. Li, J. Niu, R. Li, J. Ma, Green Chem. 13 (2011) 1238–1243.
[17] V. Polshettiwar, R.S. Varma, Org. Biomol. Chem. 7 (2009) 37–40.
[18] V. Polshettiwar, B. Baruwati, R.S. Varma, Green Chem. 11 (2009) 127–131.
[19] D. Guin, B. Baruwati, S.V. Manorama, Org. Lett. 9 (2007) 1419–1421.
[20] A.J. Amali, R.K. Rana, Green Chem. 11 (2009) 1781–1786.
[21] B. Baruwati, D. Guin, S.V. Manorama, Org. Lett. 9 (2007) 5377–5380.
[22] P.D. Stevens, G. Li, J. Fan, M. Yen, Y. Gao, Chem. Commun. (2005) 4435–4437.
[23] L. Wang, J. Bao, L. Wang, F. Zhang, Y. Li, Chem. Eur. J. 12 (2006) 6341–6347.
[24] X. Xu, X. Li, H. Gu, Z. Huang, X. Yan, Appl. Catal. A Gen. 429–430 (2012) 17–23.
[25] J.A. Baeza, L. Calvo, M.A. Gilarranz, J.J. Rodriguez, Chem. Eng. J. 240 (2014) 271–280